RECyT
Year 27 / Nº 43 / 2025 /
DOI: https://doi.org/10.36995/j.recyt.2025.43.004

Effect of operating parameters on air drying potential in a prototype dryer with heat pump

Efecto de los parámetros de funcionamiento sobre el potencial de secado del aire en un prototipo de secador con bomba de calor

Efeito dos parâmetros operacionais no potencial de secagem do ar em um protótipo de secador com bomba de calor

Rodrigo, Aparecido Jordan[1]; Fabricio, Correia de Oliveira[2, *]; Anamari, Viegas de Araújo Motomiya[1]; João, Pedro Jordan[3]; Rodrigo, Couto Santos[1]; Valdiney, Cambuy Siqueira[1]; Elton, Aparecido Siqueira Martins[1]

1- Universidade Federal da Grande Dourados. Brasil.
2- Universidade Tecnológica Federal do Paraná (UTFPR). Brasil.
3- Universidade Estadual do Oeste do Paraná (UNIOESTE). Brasil.

* E-mail: fcoliveira@utfpr.edu.br

Received: 20/08/2024; Accepted: 20/03/2025

Abstract
In low temperature drying, relative humidity —which expresses the relationship between air vapour pressure and saturation pressure at the same temperature— is the parameter with the greatest influence on the drying rate, as mass exchange is directly related to the vapour pressure difference between the product and the air. This study aimed to evaluate the effects of operating parameters on relative humidity values in a prototype system based on heat pump technology. This system was developed for low-temperature drying, cooling, and the control of air psychrometric conditions for post-harvest storage and preservation of agricultural products. The data was evaluated using a completely randomized design with five replications. Two drying temperatures were employed: 25 °C and 30 ºC. As for the air blower, rotations of 20, 25, 30, 35, 45 and 60 Hz were used. Regarding the refrigeration compressor, rotations of 30, 35, 40, 45 and 50 Hz were used. The results showed that both compressor and blower rotations had highly significant effects. On the other hand, relative humidity values tended to decrease as compressor rotation increased, whereas they increased with higher blower rotation.

Keywords: low temperature, relative humidity, cooling, evaporation temperature.

Resumen
En el secado a baja temperatura, la humedad relativa (que expresa la relación entre la presión de vapor del aire y la presión de saturación a la misma temperatura) es el parámetro que más influye en la velocidad del proceso, ya que el intercambio de masa está directamente relacionado con la diferencia de presión de vapor entre el producto y el aire. El objetivo de este trabajo fue evaluar los efectos de los parámetros de operación sobre los valores de humedad relativa en un prototipo de sistema basado en la tecnología de bomba de calor. Este sistema se desarrolló para el secado a baja temperatura, enfriamiento y control de las condiciones psicrométricas del aire para el almacenamiento poscosecha y conservación de productos agrícolas. Los datos se evaluaron mediante un diseño completamente aleatorizado con cinco repeticiones. Se utilizaron dos temperaturas de secado: 25 °C y 30 °C. Se utilizaron rotaciones del soplador de aire de 20, 25, 30, 35, 45 y 60 Hz. En cuanto al compresor de refrigeración se utilizaron rotaciones de 30, 35, 40, 45 y 50 Hz. Los resultados mostraron que tanto la rotación del compresor como la del soplador tenían efectos muy significativos. Mientras que los valores de humedad relativa tendían a disminuir al aumentar la rotación del compresor, ocurría lo contrario al aumentar la rotación del soplador.

Palabras claves: baja temperatura, humedad relativa, enfriamiento, temperatura de evaporación.

Resumo
Na secagem a baixa temperatura, a umidade relativa, que expressa a relação entre a pressão de vapor do ar e a pressão de saturação na mesma temperatura, é o parâmetro de maior influência na velocidade do processo, uma vez que a troca de massa está diretamente relacionada à diferença de pressão de vapor entre o produto e o ar. O objetivo deste trabalho foi avaliar os efeitos dos parâmetros operacionais sobre os valores de umidade relativa em um protótipo de sistema baseado na tecnologia de bomba de calor, desenvolvido para secagem a baixa temperatura, resfriamento e controle das condições psicrométricas do ar para armazenamento e conservação pós-colheita de produtos agrícolas. Os dados foram avaliados utilizando um delineamento inteiramente casualizado com cinco repetições. Foram utilizadas duas temperaturas de secagem: 25 ºC e 30 ºC. Para o insuflador de ar,

foram utilizadas as rotações de 20, 25, 30, 35, 45 e 60 Hz. Para o compressor de refrigeração, foram utilizadas rotações de 30, 35, 40, 45 e 50 Hz. Os resultados mostraram que tanto a rotação do compressor como a do insuflador tiveram efeitos altamente significativos. Enquanto os valores de umidade relativa tendem a diminuir com o aumento da rotação do compressor, o oposto acontece com o aumento da rotação do insuflador.

Palavras-chave: baixa temperatura, umidade relativa, resfriamento, temperatura de evaporação.

Introduction

The search for more efficient technologies to reduce losses, improve product quality and, equally importantly, address the environmental issue of mitigating carbon emissions is becoming increasingly important nowadays [1].

In the agricultural sector, a major consumer of energy with a large share of non-renewable sources [2], this cannot be any different. While in rural areas agricultural machinery operates practically on its own, other sectors have seen little progress, for example, the drying of agricultural products in Brazil, which is still predominantly performed using direct-burning dryers, with firewood being the most commonly used fuel [3].

In addition to product contamination with toxic and cancerous residues from direct burning [4, 5], this process also leads to the emission of greenhouse gases [6], environmental issues related to the sourcing of the wood used [7], socio-economic concerns related to land-use changes for energy crops [8]. Moreover, the combustion process in an environment laden with particulates also poses the risk of accidents related to explosions [9]. In Brazil, in recent years, there has been an increase in the number of accidents in post-harvest processing and storage units for agricultural products due to the expansion of grain production [10].

Another characteristic of wood-fired dryers is their operation with high drying temperatures, which not only increase the occurrence of physical damage [11], but also cause nutritional and sensory losses in the products [12, 13]. These factors result in storage problems and reduced market value due to loss of quality [14, 15].

In this context, heat pumps are an interesting option which make rational use of the energy, generating a thermal effect that is many times greater, as they do not convert electrical energy directly into heat, but rather transfer heat from a low-temperature source to a high-temperature source [13].

Brazil has an exceptionally clean electricity matrix, with over 87% currently sourced from renewable sources [16]. This share is continuously growing, particularly with the expansion of photovoltaic energy following the approval of laws regulating distributed generation [17]. Such regulations create a compensation system where electricity surplus can momentarily be injected into the grid and retrieved for later use, creating an even more favourable environment for the adoption of cleaner technologies, such as heat pumps.

Heat pumps stand out as very efficient equipment [18]. In addition to being environmentally friendly, as they do not use fossil fuels but high-quality energy, they are attractive for studies in drying since they offer the advantage of multiple operating controls over temperature and relative humidity. The ecological advantage of using heat pumps in drying processes lies not only in their high efficiency, but also in the precise control of temperature and relative humidity [19, 20].

While, on the one hand, reducing the temperature is beneficial for maintaining product quality [21, 22, 23, 24, 25, 26], it can also greatly extend drying time, potentially having a negative impact due to the increased energy consumption with both economic and environmental implications [27].

Therefore, in order to obtain optimal results, low-temperature drying must be performed within a brief period [28]. Unlike high temperature drying, where temperature is the determining factor in time, in low temperature drying, relative humidity is the determining factor. Therefore, the lower its value, the greater the drying potential and the shorter the as well as the less energy consumption [13].

The air supply with low relative humidity values, even at low temperatures, is another advantageous aspect of using heat pumps in drying [29]. In contrast with conventional dryers, where the air only undergoes sensible heating, heat pumps first cool the air together with a process of dehumidification and reduce its vapour pressure, then reheat it [30, 31]. In this way, low humidity values can even be obtained at low temperatures.

Another advantage of heat pumps is the possibility of full automation of all operations [32]. Being aware of how the operating parameters affect the air outlet conditions, especially the relative humidity, is important when implementing more efficient control logic. In this context, this work aimed to analyse the operation of a prototype dryer and psychrometric controller for agricultural product storage conditions based on heat pump technology, focusing on the behaviour of relative humidity as a function of the main operating parameters (compressor speed and air blower speed).

Materials and methods

The equipment used in this study, named SIARCOMPAG (Autonomous System for Cooling and Psychrometric Control of Grain Storage Conditions), is a prototype developed to modulate the psychrometric conditions of the air used in drying and post-harvest conservation of agricultural products. Its operation focuses on modulating the temperature and relative humidity of the air [33].

Constructed with pump technology, as depicted in Figures 1 and 2, the SIARCOMPAG system features an air treatment duct. Within this section, the evaporator, secondary condenser, and fan (referred to as the air blower) are located. The refrigeration compressor and primary condenser are positioned below this duct, together with their corresponding blower. Furthermore, the system is equipped with an isothermal humidifier, which has the function of incrementing both the absolute and relative humidity of the air under particular conditions. Notably, increasing the water content of the processed product is necessary only in specific use cases. Nonetheless, this action is not required when the system operates in its drying mode.

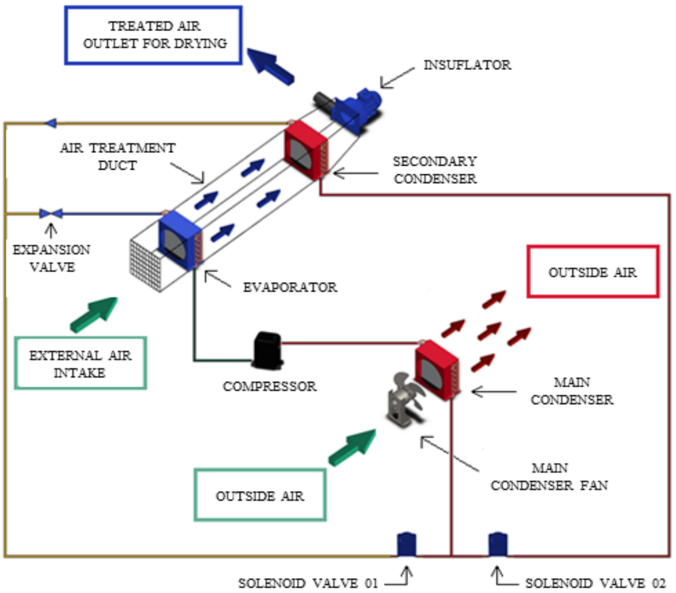

Figure 1: schematic diagram of the SIARCOMPAG.

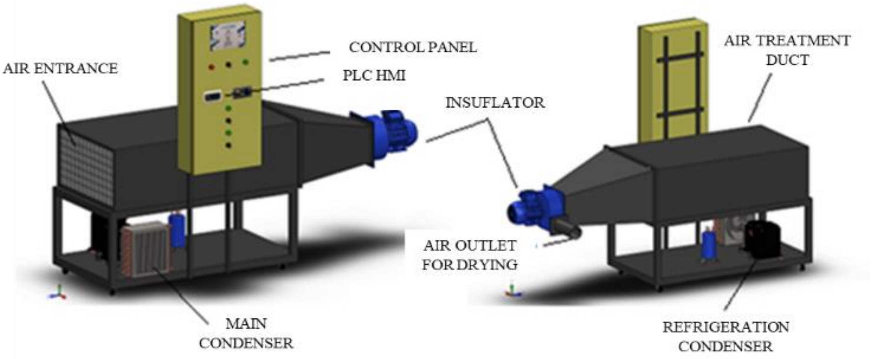

Figure 2: perspective view of the SIARCOMPAG.

The SIARCOMPAG system offers different operating modes: fully automatic, semi-automatic and fully manual. These modes can be selected and adapted based on programmable logic controller (PLC) settings through the human-machine interface (HMI). When operating in fully automatic mode, users can enter specific parameters into the HMI, including product type, desired temperature, and desired humidity of the final product. When operating in this mode, the PLC autonomously manages operating conditions by referencing equilibrium humidity equations, using PID (Proportional Integral Derivative) logic.

As for manual mode, operators are required to manually configure operational settings for each component: compressor rotation, blower rotation, auxiliary condenser activation, and main condenser fan rotation. Alternately, semi-automatic mode allows for a combination of manual and automatic adjustments. For instance, some conditions are automated, like outlet temperature, while others can be manually set.

When the system operates in drying mode, the outlet air temperature is maintained by adjusting the heat flow between the primary and secondary condensers. This is done by adjusting the rotation of the main condenser fan. Since both condensers are positioned in a sequence within the cooling circuit (an arrangement managed by the solenoid valves as depicted in Figure 1), varying the rotation of the main condenser fan adjusts the heat rejected by the secondary condenser, consequently altering the drying air temperature.

For our experiments, the system was set to semi-automatic mode: the outlet air temperature was controlled automatically, but the compressor and blower rotations were adjusted manually. In this configuration, the PLC automatically regulates the rotation of the main condenser fan to regulate the heat flow to the secondary condenser.

The drying temperatures chosen for the tests were inspired by a previous study [15], which found a correlation between drying temperature, relative humidity and drying time, revealing a direct proportionality between drying time and relative humidity. Therefore, in our study, we opted for temperatures of 25 ºC and 30 ºC, at which the relative humidity values significantly reduced the drying time.

The refrigeration compressor (Elgin model CR18K6TF5) was set to operate at rotations or frequencies of 30, 35, 40, 45, and 50 Hz. The air blower (Ventbras model SV100) was adjusted to rotations of 20, 25, 30, 35, 45, and 60 Hz. Maximums were limited to not exceeding the device's designated factory specifications. The compressor's minimum rotation was guided by manufacturer guidelines, particularly to ensure proper lubrication. The lower limit of the blower was set to prevent evaporator blockage due to potential freezing, which could be caused by an insufficient airflow rate.

Temperature and relative humidity values at the air inlet (Ent), between the evaporator and the secondary condenser (Meio), and at the air blower outlet (Saida) were supplied using the RHT sensors integrated in the SIARCOMPAG system (Figure 3), These sensors provide data on air conditions to the PLC, enabling the automatic adjustment of operating parameters.. This information can be accessed via a specific HMI (human-machine interface) screen (Figure 4).

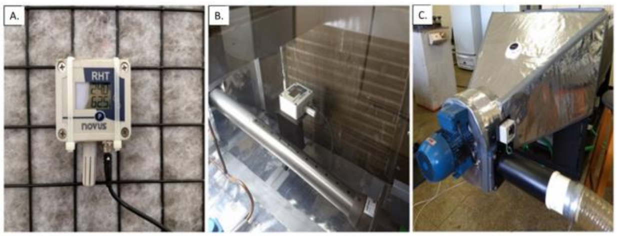

Figure 3: sensor locations: (A) RHT sensors at the entry, (B) sensor between the evaporator and secondary condenser, and (C) sensor at the air blower outlet.

Figure 4: human-machine interface screen with temperature and relative humidity data: input (Ent), midpoint (Meio) and output (Saida).

Evaporation temperatures and opening rates were supplied by the electronic expansion valve controller, which is assembled in the control panel of the psychrometric controller (Figure 5). This controller allows a highly accurate adjustment of the superheat temperature at the evaporator outlet, which facilitates operation with a practically constant evaporation temperature in each condition during the tests.

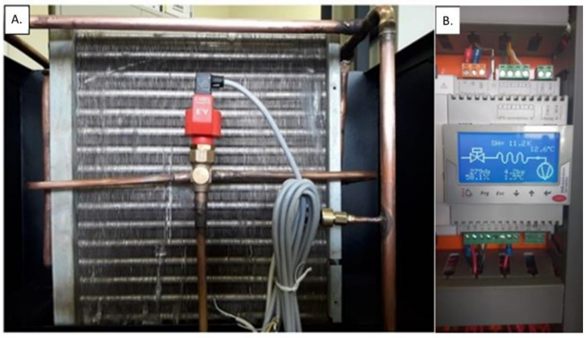

Figure 5: electronic expansion valve Carel model E^2V (A) and its corresponding controller Carel model EVD (B).

In tests where compressor rotation was adjusted, blower rotation was consistently set to its nominal value. Similarly, when blower rotation was modified, compressor rotation remained fixed at its nominal rate. For both cases, nominal rotations were equated to the maximum value employed during testing, which stood at 60 Hz.

For each setting condition, once parameters were adjusted, a stabilisation period for the equipment was observed, which ranged between 10 and 15 minutes. Upon stabilisation, measurements were taken and, to do so, each condition was subjected to five repetitions conducted at 2-minute intervals, totalling a 10-minute duration for each test.

Graphic presentations were employed to streamline the analysis, focusing on output conditions (relative humidity and temperature values) as a function of operating parameters (compressor and blower rotations).

Statistical evaluations were conducted using R statistical software, version 4.0.2 [34], based on a completely randomized design with five replications per assay. Data underwent tests to measure normality (Shapiro-Wilk test) and variance homoscedasticity (Bartlett test). After verifying these facts for each test, a variance analysis (ANOVA) was executed, gauging significance with the F test ($p \leq 0.01$).

When F values were deemed significant, data were subjected to regression analysis, evaluating both linear and polynomial models ($p \leq 0.01$). Best-fitting equations were selected based on the significance of model coefficients together with the optimal determination coefficients (R^2). As already mentioned [35], these statistical estimators effectively outline the structure of spatial dependence, which is influenced by the variables under analysis, as well as the shape and volume of the samples.

Results and discussion

Table 1 provides a summary of the variance analysis for output relative humidity values, considering both blower and compressor rotation. F-values are highly significant ($p \leq 0.01$) for both factors, indicating statistically distinct group means. The coefficient of variation (CV) is notably low, under 1%, reflecting strong experimental control and consistent data repeatability. As highlighted by Singh *et al*. [36], in agricultural research, it is preferable for CV values to be below 10%.

Table 1: F-values of the variance analysis (ANOVA) for average output relative humidity as a function of the blower and compressor rotations.

		Blower rotation			Compressor rotation	
		Drying temp. 25 °C	Drying temp. 30 °C		Drying temp. 25 °C	Drying temp. 30 °C
SV	DF	Mean squares		DF	Mean squares	
Rotation	5	114.925**	189.056**	4	50.431**	14.5536**
Error	24	0.053	0.014	20	0.049	0.0038
CV (%)		1.02	0.57		0.61	0.23

**: significant at p ≤ 0.01 for the F-test; SV: sources of variation; DF: degrees of freedom; CV: coefficient of variation.

Figure 6 shows the air conditions at the psychrometric controller inlet, representing the average temperature and relative humidity values during the tests.

Figure 7 illustrates the behaviour of the average evaporation temperature in relation to blower rotation (A) and compressor rotation (B) at drying temperatures of 25 ºC and 30 ºC. The evaporation temperature was notably influenced by these parameters. In particular, the temperature showed a direct proportionality regarding blower rotation and an inverse proportionality regarding compressor rotation.

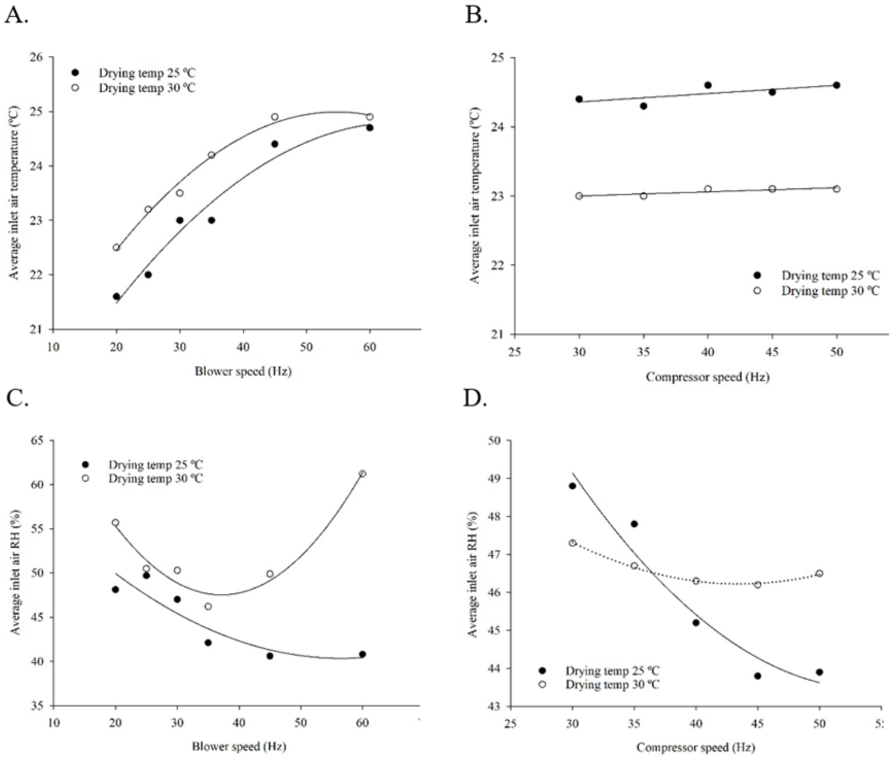

Figure 6: air conditions at the psychrometric controller inlet during tests: (A) average temperature with varied blower rotation, (B) average temperature with varied compressor rotation, (C) average relative humidity with varied blower rotation, and (D) average relative humidity with varied compressor speed.

The trend observed in the evaporation temperature in relation to the blower rotation can be attributed to the heat exchange in the evaporator and the capacity of the refrigeration system. Given that the compressor rotation remained constant, any variation in the air flow produced a change in the temperature of the evaporator outlet. This, in turn, prompted the expansion valve to avoid superheating by regulating the flow of refrigerant fluid within the evaporator. Consequently, this process altered the evaporation temperature to optimise the heat exchange process. As highlighted in a study by Wang *et al*. [37], optimizing heat exchange is crucial for heat pump systems, emphasizing the high efficiency of the dryer.

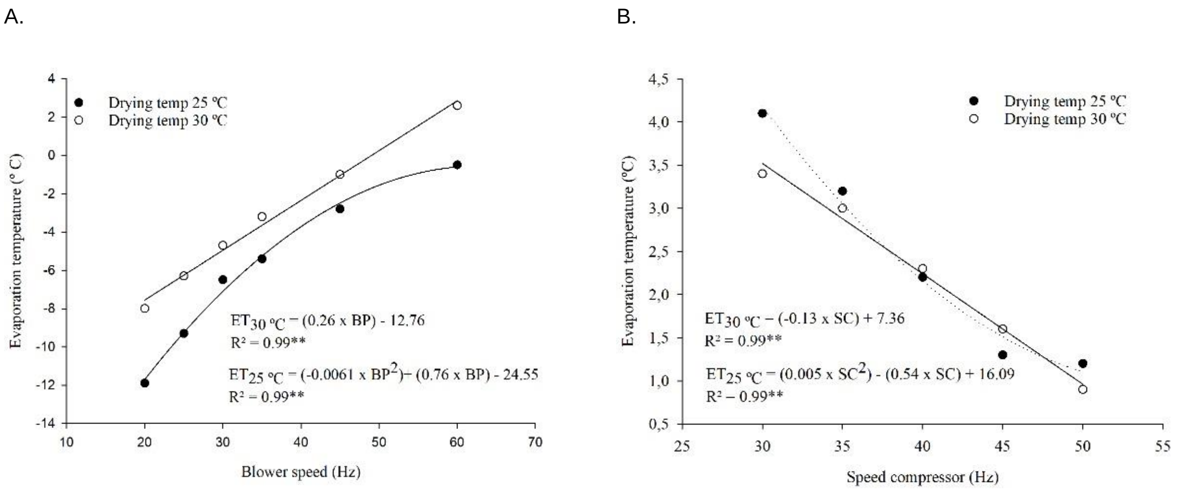

Figure 7: average evaporation temperature as a function of blower speed variation with a compressor speed fixed of 60 Hz (A) and compressor speed variation (B) with a blower speed fixed of 60 Hz.

The differences in behaviour (linear with 30 °C and second order with 25 °C) for the evaporation temperature observed in Figure 7 may be related to the difference in condensation pressure (Figure 8A), which affected the opening rate of the expansion valve (Figure 8B). The increase in drying temperature implies an increase in condensation temperature and, consequently, in condensation pressure, due to the reduction in the main condenser fan rotation to increase the heat flow that is rejected into the air in the secondary condenser.

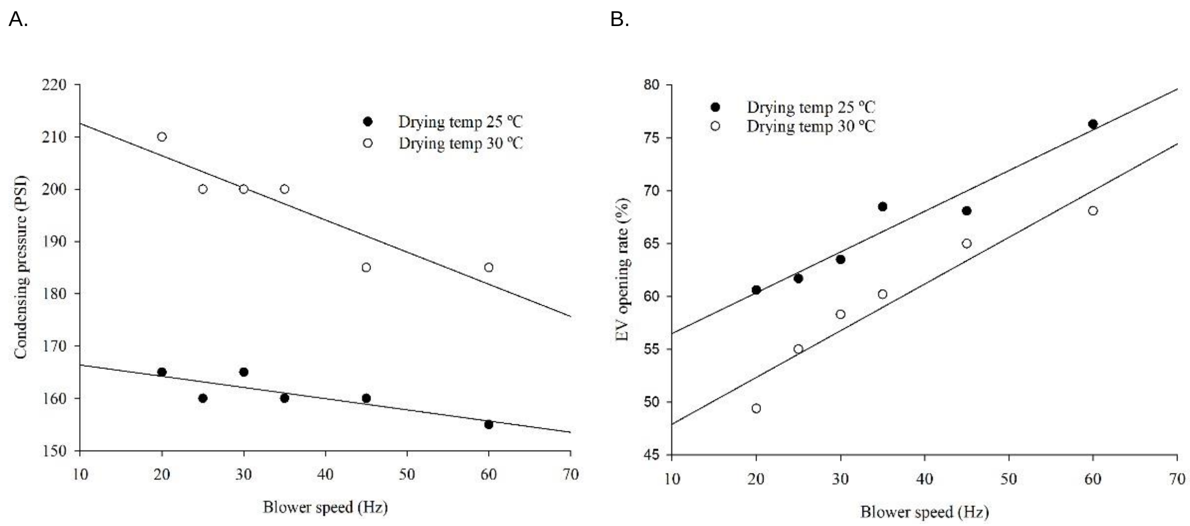

Figure 8: changes in condensing pressure (A) and expansion valve opening rate (B) as a function of varying blower rotation with compressor rotation fixed at 60 Hz.

As blower rotation increased, there was a noticeable decline in condensation pressure. This is attributed to a greater volume of air moving through the secondary condenser, enhancing the heat exchange process. Patel [38] highlighted the importance of this aspect, noting that refrigeration system performance relies significantly on efficient heat exchange, with its energy efficiency intricately linked to the pressure within the condenser.

The increase in drying temperature is achieved by reducing heat exchange in the primary condenser through a decrease in its fan speed, which in turn increases heat rejection in the secondary condenser. As the secondary condenser has a smaller capacity than the primary one, this explains the observed differences in pressure, the opening rate of the expansion valve and the slight variation in the slope inclination between the adjusted lines.

When examining the effects of changes in compressor rotation (Figure 7A), the trends in evaporation temperature appeared to be strongly associated with fluctuations in the refrigerant flow, which is controlled by the compressor. This relationship then affected the degree of opening of the expansion valve (Figure 9A). Inlet conditions during these tests were both smaller and more stable (Figures 6C and 6D). Additionally, changes in compressor rotation affected condensation pressure (Figure 9B). However, this influence was less pronounced on the opening rate of the expansion valve when the drying temperature was kept constant and only the blower rotation was varied.

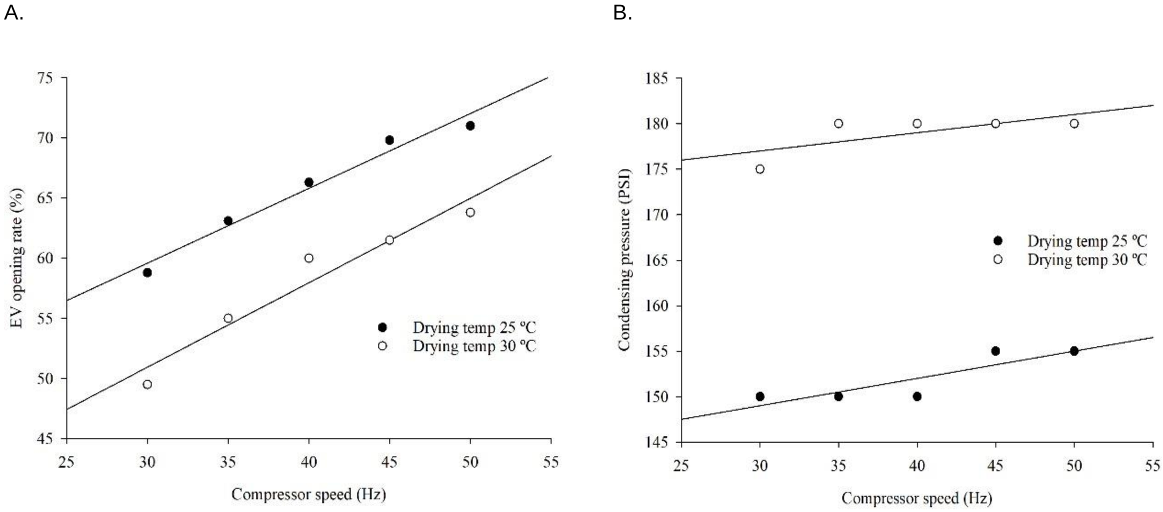

Figure 9: changes in condensing pressure (A) and expansion valve opening rate (B) as a function of varying compressor rotation with blower rotation fixed at 60 Hz.

A significant observation across both scenarios (altering blower rotation and adjusting compressor rotation) was that the opening rate of the expansion valve was higher when setting the drying temperature to 25 ºC. This trend can be attributed to the lower condensation pressure since the flow of refrigerant fluid is inherently dependent on the pressure difference between the condensation and evaporation stages. A reduced pressure difference requires the expansion valve to open further in order to maintain balanced flow.

Salazar-Hincapié et al. [18] assessed a heat pump for dehydrating aromatic herbs. They noticed that a decrease in condensation pressure was accompanied by a drop in evaporation temperature. Moreover, they further observed that an increase in condensation pressure in one of their tests resulted in greater compression work, related to the gap between the pressures during condensation and evaporation.

The variance analysis of the output relative humidity values, based on both blower and compressor rotations, showed significant results for the two assessed temperatures (Table 1). The low coefficient of variation in the results indicates an elevated level of experimental control and consistency.

Following the same trend as the evaporation temperature, the relative humidity of the air leaving the psychrometric controller tended to increase with higher blower rotation (Figure 10A) and to decrease as the compressor rotation increased (Figure 10B). This is because relative humidity values are directly related to evaporation temperature values (Figures 11 and 12) due to the cooling process with dehumidification, which takes place in the evaporator. As a consequence, the greater the cooling below the dew point, the lower the relative humidity of the air in the reheating process (outlet). Once again, the influence of compressor rotation on the pressure differential across the expansion valve becomes evident, resulting in models with different behaviour for the drying temperatures of 25 ºC and 30 ºC (Figure 10B).

A. B.

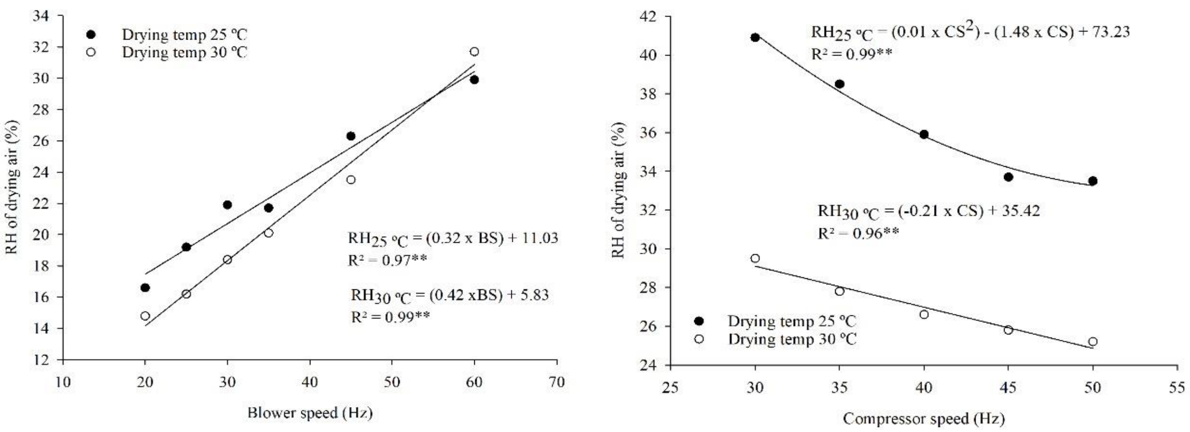

Figure 10: average output relative humidity as a function of varying blower rotation (A) at a fixed compressor rotation of 60 Hz, and (B) varying compressor rotation at a fixed blower rotation of 60 Hz.

Minimum observed values for relative humidity were 16.6% at a drying temperature of 25 ºC and 14.8% at 30 ºC. These values were observed at the lowest blower rotation while the compressor maintained a consistent rotation (Figure 10A). In a study by Aktas *et al*. [29], they achieved around 18% of relative humidity at a 36 ºC drying temperature using a recirculating heat pump dryer. Salehi [39] recorded 16% of relative humidity at 40 ºC-45 ºC during their fruit drying experiment with a heat pump. Meanwhile, Escalona *et al*. [40] recommended a minimum relative humidity of 12% for mild drying conditions at a drying temperature of 30 °C using a heat pump.

At 25 ºC, maximum values for relative humidity (40.9%) were obtained at the slowest compressor speed using a steady blower speed (Figure 10B). Meanwhile, at 30 ºC, the peak relative humidity (31.7%) was recorded at the highest blower speed with the compressor speed remaining unchanged (Figure 10A). Zlatanović *et al*. [41] reported 30% of relative humidity at 35 ºC while drying several items, including potatoes, apples, and bananas, with a heat pump. Similarly, Getahun *et al*. [42] reported approximately 35% of humidity at 50 ºC during their drying experiments with chilli peppers.

A. B.

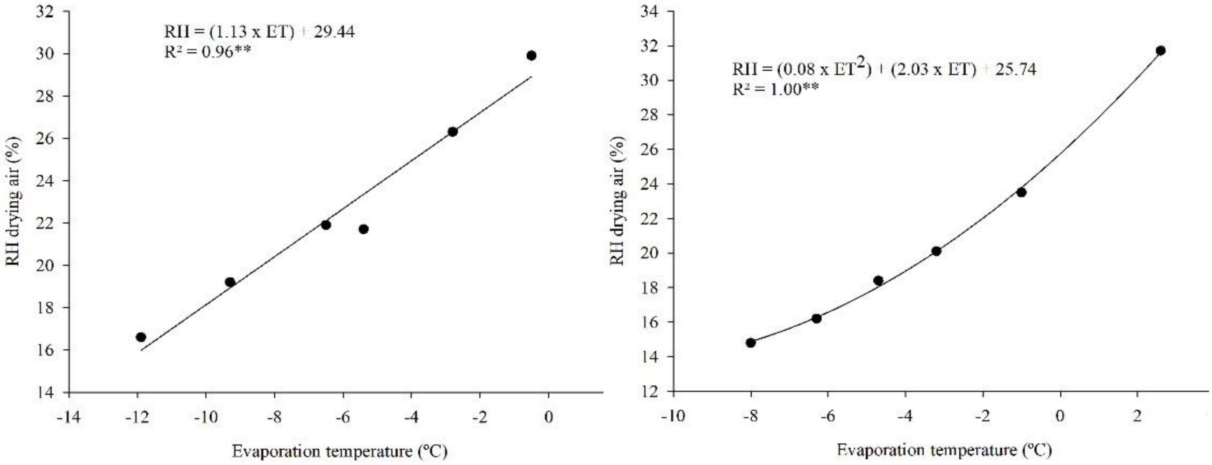

Figure 11: average relative humidity based on the evaporation temperature obtained during tests with a varying blower rotation and a fixed compressor rotation of 60 Hz: (A) drying at 25 ºC and (B) drying at 30 ºC.

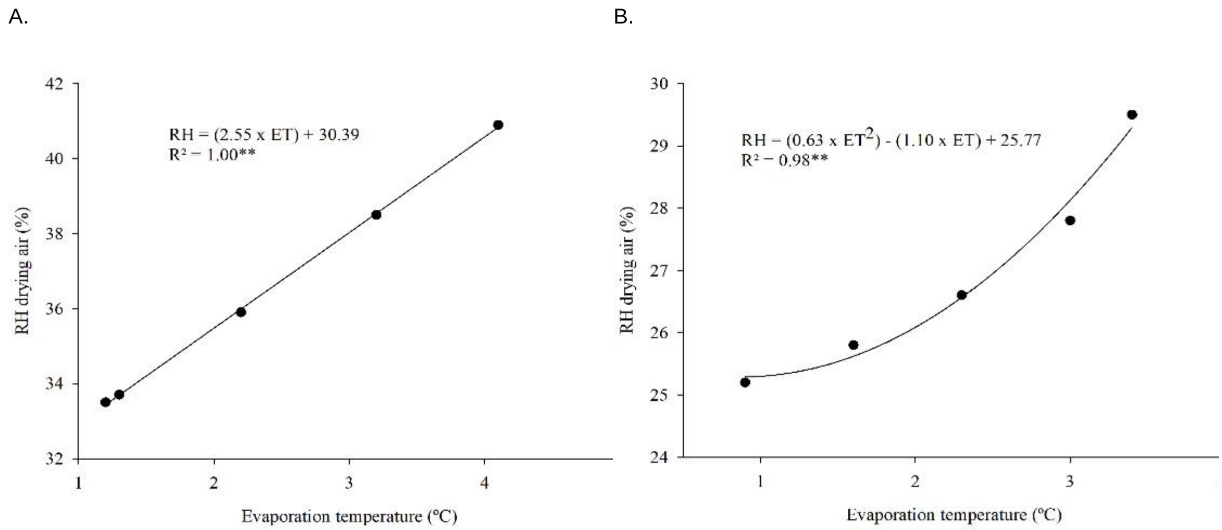

Figure 12: average relative humidity based on the evaporation temperature obtained during tests with a varying compressor rotation and a fixed blower rotation of 60 Hz: (A) drying at 25 ºC and (B) drying at 30 ºC.

The gap in relative humidity values between the two drying temperatures was more pronounced when adjusting the compressor rotation, despite only minimal variations in evaporation temperatures (Figure 7B). This suggests that the dehumidification effect associated with elevated evaporation temperatures (Figure 11) is less pronounced, implying that the primary factor in reducing relative humidity is the heating phase.

In contrast, when adjusting the blower rotation, the gap in relative humidity values between drying temperatures was narrower. Lower evaporation temperatures during the drying process of 25 ºC (Figure 10) amplified dehumidification, compensating for the decrease in relative humidity attributed to heating.

According to Zhang *et al*. [31], an increase in evaporation temperature led to a reduced drying rate, primarily due to diminished air dehumidification efficiency at higher evaporation temperatures. Mołczan & Cyklis [43] explored the effect of evaporation temperature on specific drying rates, discovering that a 10 ºC decrease in evaporation temperature enhanced water removal by more than four times, shifting from 0.44 kg kW h^{-1} to 1.90 kg kW h^{-1}.

Furthermore, Salazar-Hincapié *et al*. [18] detected challenges with ice formation in the evaporator at particularly low evaporation temperatures, which triggered heat transfer difficulties by altering the convective coefficients. Indeed, evaporator freezing is a significant issue; not only does the insulating nature of ice reduce thermal exchange, but it can also obstruct airflow.

In this study, ice buildup in the evaporator became apparent when the blower rotation dropped to 35 Hz. This accumulation hampered the heat transfer and widened the gap between the evaporator outlet and the evaporation temperature (Figure 13).

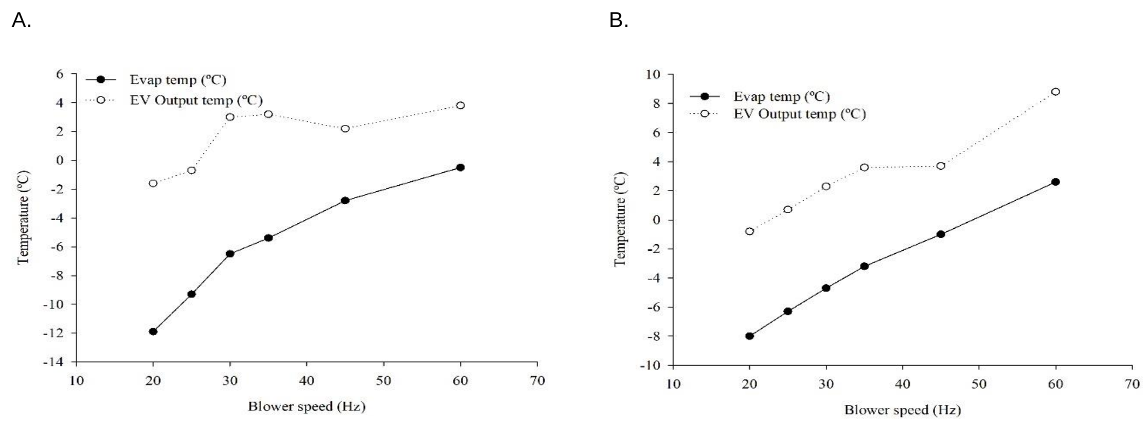

Figure 13: air temperature at the evaporator outlet as a function of evaporation temperature for different blower rotations and a fixed compressor rotation of 60 Hz: A) drying at 25 ºC and B) drying at 30 ºC.

Ice formation on the surface of the evaporator, which is more pronounced at 25 ºC (Figure 12), is a factor that may also have contributed to the differences in the slope of the adjusted lines for the linear functions, as well as to variations observed in the adjusted models (linear or quadratic).

For drying at 25 ºC (Figure 13A), assuming no ice formation and that the outlet air temperature follows the trend set by the evaporation temperature up to a blower rotation of 45 Hz, the predicted evaporator exit air temperature would be around -7 ºC with a rotation of 20 Hz. Nevertheless, due to the disruptive effect of ice on heat exchange, the actual exit temperature at this rotation was recorded as -1.7 ºC.

By modelling a scenario with an evaporator outlet air temperature of -7 ºC and then reheating it to 25 ºC, a simulation using the Grapsi v.8.1.1 software predicted an exit relative humidity of 11%. This value is considerably lower than the 16.6% observed under real conditions where ice formation occurred.

To enhance air cooling and mitigate issues related to evaporator freezing, one potential solution could be the implementation of a multi-stage cooling system. This approach could involve using a heat pump system equipped with multiple evaporators, as suggested by Du & Long [44]. By employing this strategy, the majority of the moisture in the air would be removed in the first stage, with the initial evaporator operating at a positive temperature. Subsequently, the temperature could be further reduced in the second stage with the secondary evaporator operating at sub-zero temperatures. This sequential process would not only improve the cooling efficiency but also significantly reduce the probability of ice formation.

Conclusions

1. Varying compressor and blower rotations, even with a constant drying temperature, resulted in a variation of almost 40% in relative humidity values of the outlet air.

2. Increasing the compressor rotation from 30 Hz to 50 Hz produced a reduction of nearly 20% in the relative humidity values, whereas increasing the blower speed from 20 Hz to 60 Hz led to an approximate 50% increase. Therefore, lower blower rotations and higher compressor rotations help to reduce relative humidity values and, consequently, increase the drying potential of the air.

3. Varying the blower rotation implied a greater variation in relative humidity values, due to an existing correlation between relative humidity and evaporation temperature — lower evaporation temperatures resulted in lower relative humidity values. Consequently, the reduction in air flow produced a decrease in evaporation temperature values.

4. Decreasing temperature and air flow rate, combined with an increasing compressor rotation (that is to say, a greater mass flow of refrigerant), produced more efficient heat exchange, ensuring that the air is cooled below the dew point. The greater the degree of cooling below the dew point, the more water is removed, resulting in lower absolute humidity and lower vapour pressure. As a result, after the reheating stage, the relative humidity of the air is reduced, thereby enhancing its drying potential at the same temperature.

5. On the other hand, reducing the blower rotation below 35 Hz caused the evaporation temperature to drop below 0 °C, leading to ice formation and accumulation in the evaporator. This consequence interfered with the downward behaviour of the relative humidity values of the drying air.

Acknowledgments

We express our deep gratitude to the *Programa de Pós-Graduação em Engenharia Agrícola* at the *Universidade Federal da Grande Dourados* (PGEA/UFGD). We extend our sincere gratitude to the Coordenação de Aperfeiçoamento de Pessoal de Nível Superior (CAPES—Finance Code: PDPG 155 and 16/2022) for their financial support. We would also like to thank the team at STTA for their valuable feedback and review of the definitive version of this article.

Reference

1. **Rawat, A., Kumar, D., & Khati, B. S**. (2024). *A review on climate change impacts, models, and its consequences on different sectors: A systematic approach*. Journal of Water and Climate Change, 15(1), 104-126. https://doi.org/10.2166/wcc.2023.536

2. **Guimarães, G.; Arcanjo, A.** *Os benefícios da energia solar em propriedades rurais*. 2019. SolarVolt Energia. [SolarVolt]. Disponível em:

https://www.solarvoltenergia.com.br/blog/energia-solar-em-propriedades-rurais/. Acesso em: 8 ago. 2023.

3. **Cortez, L. A. B., Lora, E. E. S., Gomez, E. O.**, 2008. *Biomassa para energia*. Campinas, SP: Editora UNICAMP.

4. **Lima, R. F., Dionello, R. G., Peralba, M. C. R., Barrionuevo, S., Radunz, L. L., Reichert Júnior, F. W.**, 2017. *PAHs in corn grains submitted to drying with firewood*. Food Chemistry. 215, 165–170.

5. **Resende, O.; Costa, E. R.; Quequeto, W. D.; Costa, L. M.; Oliveira, D. E. C.; Tfouni, S. A. V.; Gomes, F. M. L.; Quirino, J. R.; Lima, R. R.** *Quality of corn grains subjected to drying using direct-fired furnace fed with eucalyptus chips and firewood*. Food Sci. Technol, Campinas, v42, e55820, 2022. https://doi.org/10.1590/fst.55820.

6. **Bilandzija, N.; Voca, N.; Jelcic, B.; Jurisic, V.; Grubor, M.; Kricka, T.** 2018. *Evaluation of Croatian agricultural solid biomass energy potential*. Renewable and Sustainable Energy Reviews 93, 225–230.

7. **Seiffert, M. E. B.** *Mercado de Carbono e Protocolo de Quioto: Oportunidades de negócio na busca da sustentabilidade.* 2. ed. São Paulo: Atlas, 2013.

8. **Lourenzani, W. L.; Caldas, M. M.** *Mudanças no uso da terra decorrentes da expansão da cultura da cana-de-açúcar na região oeste do estado de São Paulo*. Ciência Rural, Santa Maria, v.44, n.11, p.1980-987, nov, 2014. https://doi.org/10.1590/0103-8478cr20140186 .

9. **Zaperllon, L. E.; Morejon, C. F. M.** *Estudo prospectivo dos incêndios e explosões em unidades industriais de beneficiamento e armazenamento de grãos no estado do Paraná*. Revista Científica do Corpo de Bombeiros Militar de Pernambuco. Vol.04 Nº11 - Edição Especial XVIII SENABOM, novembro de 2018. http://dx.doi.org/10.17648/2359-4837/flammae.v4n11.p155-169.

10. **Ferreira, R. A.; Martinazzo, A. P.** *Levantamento de acidentes de trabalho em unidades armazenadoras brasileiras no período de 2011/2021*. Revista Thêma et Scientia – Vol. 13, no 1, jan/jun 2023.

11. **Mabasso, G. A.; Siqueira, V. C.; Resende, O.; Quequeto, W. D.; Goneli, A. L. D.; Martins, E. A. S.; Takagi, A. D. A.** *Mechanical properties and integrity of stored corn grains after continuous and intermittent drying*. Food Sci. Technol, Campinas, 43, e21323, 2023. Food Sci. Technol, Campinas, 43, e21323, 2023. https://doi.org/10.5327/fst.21323.

12. **Schiavon, R. A.; Castro, L. K.; Borges, G. B.; Nogueira, I. S.; Silva, R. V.** *Efeito da temperatura de secagem sobre a qualidade dos grãos de soja*. Anais da VII Conferência Brasileira de Pós-colheita e X Simpósio Paranaense de Pós-colheita de grãos. 16 a 18 de outubro de 2018. Londina-PR. Disponível em: https://eventos.abrapos.org.br/anais/paperfile/910_20181103_02-43-42_832.pdf. Acesso em: 12 jul 2024.

13. **Jordan, R. A., Siqueira, V. C., Quequeto, W. D., Cavalcanti-Mata, M. E. R. M., Hoscher, R. H., Mabasso, G. A., Battilani, M., Oliveira, F. C. de, Martins, E. A. S. & Freitas, R. L.** (2020). *Consumo específico de energia na secagem de café com sistema de aquecimento resistivo e bomba de calor*. Research, Society and Development, 9(9), e303997297-e303997297. doi: 10.33448/rsd-v9i9.7297

14. **Alves, G. E., Borém, F. M., Isquierdo, E. P., Siqueira, V. C., Cirillo, M. A., Pinto, A. C. F.** (2017). *Physiological and sensorial quality of Arabica coffee subjected to different temperatures and drying airflows*. Acta Scientiarum. Agronomy, 39(2), 225-233.

15. **Borém, F. M.; Isquierdo, E. P.; Alves, G. E.; Ribeiro, D. E.; Siqueira, V. C.; Taveira, J. H. Da. S.** *Quality of natural coffee dried under different temperatures and drying rates*. Coffee Science, v.13, n.2, p.159-167, 2018. http://dx.doi.org/10.25186/cs.v13i2.1410

16. **EPE [Empresa de Pesquisa Energética]**. *Balanço Energético Nacional (BEN) 2024/Relatório síntese: Ano base 2023*. Disponível em https://www.epe.gov.br/sites-pt/publicacoes-dados-abertos/publicacoes/PublicacoesArquivos/publicacao-819/topico-715/BEN_S%C3%ADntese_2024.pdf. Acesso em: jun/2024.

17. **BRASIL**. *LEI No 14.300, DE 6 DE JANEIRO DE 2022 - DOU - Imprensa Nacional*. 6 jan. 2022. Portal da Imprensa Nacional do Brasil. Diário Oficial da União. Disponível em: https://in.gov.br/en/web/dou/-

/lei-n-14.300-de-6-de-janeiro-de-2022-372467821. Acesso em: 28 ago. 2023. (Brasília, DF).

18. Salazar-Hincapié, A.; Delgado-Mejía, A; Romero-Maya, A. F.; Duque-Grisales, E. *Experimental assessment of the thermal performance of a heat pump dryer system based on the variations in compressor discharge pressure on oregano drying*. Energies, v.13, p.6333, 2020. https://doi.org/10.3390/en13236333

19. Budžaki, S.; Leko, J.; Jovanović, K.; Viszmeg, J.; Koški, I. *Air Source Heat Pump Assisted Drying for Food Applications*. Croatian Journal of Food Science and Technology, v.11, p.122-130, 2019. https://doi.org/10.17508/CJFST.2019.11.1.18

20. Loemba, A. B. T.; Kichonge, B.; Kivevele, T. *Comprehensive assessment of heat pump dryers for drying agricultural products*. Energy Science & Engineering, v.11, n.8, p.2985-3014, 2023. https://doi.org/10.1002/ese3.1326

21. Montoya-Ballesteros, L. C.; González-León, A.; Martínez-Núnez, Y. J.; Robles-Burgueno, M. R.; García-Alvarado, M. A.; Rodríguez-Jimenes, G. C. *Impact of open sun drying and hot air drying on capsaicin, capsanthin, and ascorbic acid content in chiltepin (Capsicum annuum L. var. glabriusculum)*. Revista Mexicana de Ingeniera Quimica, v.16, p.813-825, 2017.

22. Verruck, S.; Prudencio, E. S.; da Silveira, S. M. *Compostos bioativos com capacidade antioxidante e antimicrobiana em frutas.* Revista CSBEA, v.4, n.1, p.111-124, 2018. https://doi.org/10.5965/24473650412018111

23. Gasecka M.; Siwulski M.; Magdziak Z.; Budzynska S.; Stuper-Szablewska K.; Niedzielski P.; Mleczek, M. *The effect of drying temperature on bioactive compounds and antioxidant activity of Leccinum scabrum (Bull.) Gray and Hericium erinaceus (Bull.) Pers*. Journal of Food Science and Technology, v.57, n.2, p.513-525, 2020. https://doi.org/10.1007/s13197-019-04081-1

24. Ashok, K. M.; Rajakarunakaran, S.; Kumaresan, G. *Performance Evaluation of Heat Pump Dryer in Specific Moisture Evaporation Rate for Various Herbal Leaves*. International Journal of Engineering Research & Technology (IJERT), v.10, n.7, p.616-620, 2021.

25. Gou, M.; Bi, J.; Chen, Q.; Wu, X.; Fauconnier, M-L.; Qiao, Y. *Advances and Perspectives in Fruits and Vegetables Flavor Based on Molecular Sensory Science*. Food Reviews International, v.39, p.3066-3079, 2021 https://doi.org/10.1080/87559129.2021.2005088

26. Xu, L.; Zang, E.; Sun, S.; Li, M. *Main flavor compounds and molecular regulation mechanisms in fruits and vegetables*. Critical Reviews in Food Science and Nutrition, p.1-2, 2022. https://doi.org/10.1080/10408398.2022.2097195

27. Tajudin, N. H. A.; Ang, W. L.; Tasirin, S. M.; Rosli, M. I. *Process variables optimization for heat pump drying of roselle calyx by using response surface methodology*. Jurnal Kejuruteraan, v.33, n.4, p.903-914, 2021. https://doi.org/10.17576/jkukm-2021-33(4)-13

28. ElGamal, R.; Song, C.; Rayan, A. M.; Liu, C.; Al-Rejaie, S.; ElMasry, G. *Thermal Degradation of Bioactive Compounds during Drying Process of Horticultural and Agronomic Products: A Comprehensive Overview*. Agronomy, v.13, n.6, p.1580. https://doi.org/10.3390/agronomy13061580

29. Aktaş, M.; Taşeri, L.; Şevik, S.; Gülcü, M.; Uysal Seçkin, G.; Dolgun, E. C. *Heat pump drying of grape pomace: Performance and product quality analysis*. Drying Technology, v.37, n.14, p.1766-1779, 2019. https://doi.org/10.1080/07373937.2018.1536983

30. Uthpala, T. G. G.; Navaratne, S. B.; Thibbotuwawa, A. *Review on low-temperature heat pump drying applications in food industry: Cooling with dehumidification drying method*. Jouranl of Food Process Engineering, v.43, p.e13502, 2020. https://doi.org/10.1111/jfpe.13502

31. Zhang, T.; Yan, Z. W.; Wang, L.Y.; Zheng, W.J.; Wu, Q.; Meng, Q. L. *Theoretical analysis and experimental study on a low-temperature heat pump sludge drying system*. Energy, v.214, p.118985, 2021. https://doi.org/10.1016/j.energy.2020.118985

32. Liu, Y., Zhao, K., Jiu, M., & Zhang, Y. (2017). *Design and drying technology research of heat pump Lentinula edodes* *drying room*. Procedia Engineering, 205(1), 983-988.

33. Jordan, R. A.; Siqueira, V. C.; Cavalcanti-Mata, M. E. R. M.; Hoscher, R. H.; Mabasso, G. A.; Quequeto, W. D.; Battilani, M.; Freitas, R. L.; Oliveira, F. C.; Martins, E. A. S. *Qualidade sensorial do café submetido a secagem a baixa temperatura e a frio com emprego de um sistema baseado em tecnologia de bomba de calor*. Research, Society and Development, v.9, n.11, p.e59791110302, 2020. https://doi.org/10.33448/rsd-v9i11.10302

34. R Core Team. *R: A language and environment for statistical computing. Vienna: R Foundation for Statistical Computing*, 2017. Available on: <https://www.r-project.org/>. Accessed on: Set. 2023.

35. Silva, N. C. D.; Santos, R. C.; Zucca, R.; Geisenhoff, L. O.; Cesca, R. S.; Lovatto, J. *Enthalpy thematic map interpolated with spline method for management of broiler chicken production*. Revista Brasileira de Engenharia Agrícola e Ambiental, v.24, p.431-436. https://doi.org/10.1590/1807-1929/agriambi.v24n7p431-436

36. Singh, A.; Sharma, J.; Paichha, M.; Chakrabarti, R., 2020. *Achyranthes aspera (prickly chaff flower) leaves- and seeds-supplemented diets regulate growth, innate immunity, and oxidative stress in Aeromonas hydrophila-challenged Labeo rohita*. J. Appl. Aquacult., 32 (3): 250-267

37. Wang, C.; Gao, Y.; Dai, Z.; Wu, D.; Huang, Z.; Zhang, X.; Jiang, L. *Experimental investigation and performance evaluation on a direct expansion solar-air source heat pump system*. International Journal of Refrigeration, v.145, p.168-176, 2023. https://doi.org/10.1016/j.ijrefrig.2022.08.030

38. Patel, A. *Enhancing Heat Transfer Efficiency in Solar Thermal Systems Using Advanced Heat Exchangers*. Multidisciplinary International Journal of Research and Development (MIJRD), v.2. n.06, p.31-51, 2023. https://www.mijrd.com/papers/v2/i6/MIJRDV2I60003.pdf

39. Salehi, F. *Recent applications of heat pump dryer for drying of fruit crops: A review*. International Journal of Fruit Science, v.21, n.1, p.546-555, 2021. https://doi.org/10.1080/15538362.2021.1911746

40. Escalona, A.; Cuevas, C.; Salazar, L.; Hernandez, V. *Modelling of heat pump drying system powered by a hybrid PV-wind-battery plant for slow-drying hardwoods*. Energy for Sustainable Development, v.76, p.101282, 2023. https://doi.org/10.1016/j.esd.2023.101282

41. Zlatanović, I.; Komatina, M.; Antonijević, D. *Experimental investigation of the efficiency of heat pump drying system with full air recirculation*, Journal of Food Process Engineering, v.40, n.2, 2017. https://doi.org/10.1111/jfpe.12386

42. Getahun, E.; Delele, M. A.; Gabbiye, N.; Fanta, S. W.; Vanierschot, M. *Studying the drying characteristics and quality attributes of chili pepper at different maturity stages: experimental and mechanistic model*. Case Studies in Thermal Engineering, v.26, p.101052, 2021. https://doi.org/10.1016/j.csite.2021.101052

43. Mołczan, T.; Cyklis, P. *Impact of the evaporation temperature on the air-drying rate for a finned heat exchanger*. Energies, v.16, n.5, p.2132, 2023. https://doi.org/10.3390/en16052132

44. Du, A.; Long, J. *Heating performance of a novel two-stage evaporator air-source heat-pump for drying applications*. Dry Technol, v.40, p.1356-1368, 2022. https://doi.org/10.1080/07373937.2020.1869036